

**Search for a Higgs Boson in the Diphoton Final State
in $p\bar{p}$ Collisions at $\sqrt{s} = 1.96$ TeV**

T. Aaltonen,²¹ B. Álvarez González^{w,9}, S. Amerio,⁴¹ D. Amidei,³² A. Anastassov,³⁶ A. Annovi,¹⁷ J. Antos,¹²
G. Apollinari,¹⁵ J.A. Appel,¹⁵ A. Apresyan,⁴⁶ T. Arisawa,⁵⁶ A. Artikov,¹³ J. Asaadi,⁵¹ W. Ashmanskas,¹⁵
B. Auerbach,⁵⁹ A. Aurisano,⁵¹ F. Azfar,⁴⁰ W. Badgett,¹⁵ A. Barbaro-Galtieri,²⁶ V.E. Barnes,⁴⁶ B.A. Barnett,²³
P. Barria^{dd,44} P. Bartos,¹² M. Bauce^{bb,41} G. Bauer,³⁰ F. Bedeschi,⁴⁴ D. Beecher,²⁸ S. Behari,²³ G. Bellettini^{cc,44}
J. Bellinger,⁵⁸ D. Benjamin,¹⁴ A. Beretvas,¹⁵ A. Bhatti,⁴⁸ M. Binkley,^{15,*} D. Bisello^{bb,41} I. Bizjak^{hh,28} K.R. Bland,⁵
B. Blumenfeld,²³ A. Bocci,¹⁴ A. Bodek,⁴⁷ D. Bortoletto,⁴⁶ J. Boudreau,⁴⁵ A. Boveia,¹¹ L. Brigliadori^{aa,6}
A. Brisuda,¹² C. Bromberg,³³ E. Brucken,²¹ M. Bucchiantonio^{cc,44} J. Budagov,¹³ H.S. Budd,⁴⁷ S. Budd,²²
K. Burkett,¹⁵ G. Busetto^{bb,41} P. Bussey,¹⁹ A. Buzatu,³¹ C. Calancha,²⁹ S. Camarda,⁴ M. Campanelli,²⁸
M. Campbell,³² F. Canelli^{11,15} B. Carls,²² D. Carlsmith,⁵⁸ R. Carosi,⁴⁴ S. Carrillo^{k,16} S. Carron,¹⁵ B. Casal,⁹
M. Casarsa,¹⁵ A. Castro^{aa,6} P. Catastini,²⁰ D. Cauz,⁵² V. Cavaliere,²² M. Cavalli-Sforza,⁴ A. Cerri^{e,26}
L. Cerrito^{q,28} Y.C. Chen,¹ M. Chertok,⁷ G. Chiarelli,⁴⁴ G. Chlachidze,¹⁵ F. Chlebana,¹⁵ K. Cho,²⁵
D. Chokheli,¹³ J.P. Chou,²⁰ W.H. Chung,⁵⁸ Y.S. Chung,⁴⁷ C.I. Ciobanu,⁴² M.A. Ciocci^{dd,44} A. Clark,¹⁸
C. Clarke,⁵⁷ G. Compostella^{bb,41} M.E. Convery,¹⁵ J. Conway,⁷ M. Corbo,⁴² M. Cordelli,¹⁷ C.A. Cox,⁷ D.J. Cox,⁷
F. Crescioli^{cc,44} C. Cuenca Almenar,⁵⁹ J. Cuevas^{w,9} R. Culbertson,¹⁵ D. Dagenhart,¹⁵ N. d'Ascenzo^{u,42}
M. Datta,¹⁵ P. de Barbaro,⁴⁷ S. De Cecco,⁴⁹ G. De Lorenzo,⁴ M. Dell'Orso^{cc,44} C. Deluca,⁴ L. Demortier,⁴⁸
J. Deng^{b,14} M. Deninno,⁶ F. Devoto,²¹ M. d'Errico^{bb,41} A. Di Canto^{cc,44} B. Di Ruzza,⁴⁴ J.R. Dittmann,⁵
M. D'Onofrio,²⁷ S. Donati^{cc,44} P. Dong,¹⁵ M. Dorigo,⁵² T. Dorigo,⁴¹ K. Ebina,⁵⁶ A. Elagin,⁵¹ A. Eppig,³²
R. Erbacher,⁷ D. Errede,²² S. Errede,²² N. Ershaidat^{z,42} R. Eusebi,⁵¹ H.C. Fang,²⁶ S. Farrington,⁴⁰ M. Feindt,²⁴
J.P. Fernandez,²⁹ C. Ferrazza^{ee,44} R. Field,¹⁶ G. Flanagan^{s,46} R. Forrest,⁷ M.J. Frank,⁵ M. Franklin,²⁰
J.C. Freeman,¹⁵ Y. Funakoshi,⁵⁶ I. Furic,¹⁶ M. Gallinaro,⁴⁸ J. Galyardt,¹⁰ J.E. Garcia,¹⁸ A.F. Garfinkel,⁴⁶
P. Garosi^{dd,44} H. Gerberich,²² E. Gerchtein,¹⁵ S. Giagu^{ff,49} V. Giakoumopoulou,³ P. Giannetti,⁴⁴ K. Gibson,⁴⁵
C.M. Ginsburg,¹⁵ N. Giokaris,³ P. Giromini,¹⁷ M. Giunta,⁴⁴ G. Giurgiu,²³ V. Glagolev,¹³ D. Glenzinski,¹⁵
M. Gold,³⁵ D. Goldin,⁵¹ N. Goldschmidt,¹⁶ A. Golossanov,¹⁵ G. Gomez,⁹ G. Gomez-Ceballos,³⁰ M. Goncharov,³⁰
O. González,²⁹ I. Gorelov,³⁵ A.T. Goshaw,¹⁴ K. Goulianos,⁴⁸ S. Grinstein,⁴ C. Grosso-Pilcher,¹¹ R.C. Group^{55,15}
J. Guimaraes da Costa,²⁰ Z. Gunay-Unalan,³³ C. Haber,²⁶ S.R. Hahn,¹⁵ E. Halkiadakis,⁵⁰ A. Hamaguchi,³⁹
J.Y. Han,⁴⁷ F. Happacher,¹⁷ K. Hara,⁵³ D. Hare,⁵⁰ M. Hare,⁵⁴ R.F. Harr,⁵⁷ K. Hatakeyama,⁵ C. Hays,⁴⁰ M. Heck,²⁴
J. Heinrich,⁴³ M. Herndon,⁵⁸ S. Hewamanage,⁵ D. Hidas,⁵⁰ A. Hocker,¹⁵ W. Hopkins^{f,15} D. Horn,²⁴ S. Hou,¹
R.E. Hughes,³⁷ M. Hurwitz,¹¹ U. Husemann,⁵⁹ N. Hussain,³¹ M. Hussein,³³ J. Huston,³³ G. Introzzi,⁴⁴ M. Iori^{ff,49}
A. Ivanov^{o,7} E. James,¹⁵ D. Jang,¹⁰ B. Jayatilaka,¹⁴ E.J. Jeon,²⁵ M.K. Jha,⁶ S. Jindariani,¹⁵ W. Johnson,⁷
M. Jones,⁴⁶ K.K. Joo,²⁵ S.Y. Jun,¹⁰ T.R. Junk,¹⁵ T. Kamon,⁵¹ P.E. Karchin,⁵⁷ A. Kasmi,⁵ Y. Kato^{n,39}
W. Ketchum,¹¹ J. Keung,⁴³ V. Khotilovich,⁵¹ B. Kilminster,¹⁵ D.H. Kim,²⁵ H.S. Kim,²⁵ H.W. Kim,²⁵ J.E. Kim,²⁵
M.J. Kim,¹⁷ S.B. Kim,²⁵ S.H. Kim,⁵³ Y.K. Kim,¹¹ N. Kimura,⁵⁶ M. Kirby,¹⁵ S. Klimenko,¹⁶ K. Kondo,^{56,*}
D.J. Kong,²⁵ J. Konigsberg,¹⁶ A.V. Kotwal,¹⁴ M. Kreps,²⁴ J. Kroll,⁴³ D. Krop,¹¹ N. Krumnack^{l,5} M. Kruse,¹⁴
V. Krutelyov^{c,51} T. Kuhr,²⁴ M. Kurata,⁵³ S. Kwang,¹¹ A.T. Laasanen,⁴⁶ S. Lami,⁴⁴ S. Lammel,¹⁵ M. Lancaster,²⁸
R.L. Lander,⁷ K. Lannon^{v,37} A. Lath,⁵⁰ G. Latino^{cc,44} T. LeCompte,² E. Lee,⁵¹ H.S. Lee,¹¹ J.S. Lee,²⁵ S.W. Lee^{x,51}
S. Leo^{cc,44} S. Leone,⁴⁴ J.D. Lewis,¹⁵ A. Limosani^{r,14} C.-J. Lin,²⁶ J. Linacre,⁴⁰ M. Lindgren,¹⁵ E. Lipeles,⁴³
A. Lister,¹⁸ D.O. Litvintsev,¹⁵ C. Liu,⁴⁵ Q. Liu,⁴⁶ T. Liu,¹⁵ S. Lockwitz,⁵⁹ A. Loginov,⁵⁹ D. Lucchesi^{bb,41}
J. Lueck,²⁴ P. Lujan,²⁶ P. Lukens,¹⁵ G. Lungu,⁴⁸ J. Lys,²⁶ R. Lysak,¹² R. Madrak,¹⁵ K. Maeshima,¹⁵
K. Makhoul,³⁰ S. Malik,⁴⁸ G. Manca^{a,27} A. Manousakis-Katsikakis,³ F. Margaroli,⁴⁶ C. Marino,²⁴ M. Martínez,⁴
R. Martínez-Ballarín,²⁹ P. Mastrandrea,⁴⁹ M.E. Mattson,⁵⁷ P. Mazzanti,⁶ K.S. McFarland,⁴⁷ P. McIntyre,⁵¹
R. McNulty^{i,27} A. Mehta,²⁷ P. Mehtala,²¹ A. Menzione,⁴⁴ C. Mesropian,⁴⁸ T. Miao,¹⁵ D. Mietlicki,³² A. Mitra,¹
H. Miyake,⁵³ S. Moed,²⁰ N. Moggi,⁶ M.N. Mondragon^{k,15} C.S. Moon,²⁵ R. Moore,¹⁵ M.J. Morello,¹⁵ J. Morlock,²⁴
P. Movilla Fernandez,¹⁵ A. Mukherjee,¹⁵ Th. Muller,²⁴ P. Murat,¹⁵ M. Mussini^{aa,6} J. Nachtman^{m,15} Y. Nagai,⁵³
J. Naganoma,⁵⁶ I. Nakano,³⁸ A. Napier,⁵⁴ J. Nett,⁵¹ C. Neu,⁵⁵ M.S. Neubauer,²² J. Nielsen^{d,26} L. Nodulman,²
O. Norriella,²² E. Nurse,²⁸ L. Oakes,⁴⁰ S.H. Oh,¹⁴ Y.D. Oh,²⁵ I. Oksuzian,⁵⁵ T. Okusawa,³⁹ R. Orava,²¹
L. Ortolan,⁴ S. Pagan Griso^{bb,41} C. Pagliarone,⁵² E. Palencia^{e,9} V. Papadimitriou,¹⁵ A.A. Paramonov,²
J. Patrick,¹⁵ G. Pauletta^{gg,52} M. Paulini,¹⁰ C. Paus,³⁰ D.E. Pellett,⁷ A. Penzo,⁵² T.J. Phillips,¹⁴ G. Piacentino,⁴⁴
E. Pianori,⁴³ J. Pilot,³⁷ K. Pitts,²² C. Plager,⁸ L. Pondrom,⁵⁸ S. Poprocki^{f,15} K. Potamianos,⁴⁶ O. Poukhov,^{13,*}

F. Prokoshin^{y,13} A. Pronko,¹⁵ F. Ptohos^{g,17} E. Pueschel,¹⁰ G. Punzi^{cc,44} J. Pursley,⁵⁸ A. Rahaman,⁴⁵
 V. Ramakrishnan,⁵⁸ N. Ranjan,⁴⁶ J. Ray,¹⁵ I. Redondo,²⁹ P. Renton,⁴⁰ M. Rescigno,⁴⁹ T. Riddick,²⁸ F. Rimondi^{aa,6},
 L. Ristori^{44,15} A. Robson,¹⁹ T. Rodrigo,⁹ T. Rodriguez,⁴³ E. Rogers,²² S. Rolli^{h,54} R. Roser,¹⁵ M. Rossi,⁵²
 F. Rubbo,¹⁵ F. Ruffini^{dd,44} A. Ruiz,⁹ J. Russ,¹⁰ V. Rusu,¹⁵ A. Safonov,⁵¹ W.K. Sakumoto,⁴⁷ Y. Sakurai,⁵⁶
 L. Santi^{gg,52} L. Sartori,⁴⁴ K. Sato,⁵³ V. Saveliev^{u,42} A. Savoy-Navarro,⁴² P. Schlabach,¹⁵ A. Schmidt,²⁴
 E.E. Schmidt,¹⁵ M.P. Schmidt,^{59,*} M. Schmitt,³⁶ T. Schwarz,⁷ L. Scodellaro,⁹ A. Scribano^{dd,44} F. Scuri,⁴⁴
 A. Sedov,⁴⁶ S. Seidel,³⁵ Y. Seiya,³⁹ A. Semenov,¹³ F. Sforza^{cc,44} A. Sfyrla,²² S.Z. Shalhout,⁷ T. Shears,²⁷
 P.F. Shepard,⁴⁵ M. Shimojima^{t,53} S. Shiraishi,¹¹ M. Shochet,¹¹ I. Shreyber,³⁴ A. Simonenko,¹³ P. Sinervo,³¹
 A. Sissakian,^{13,*} K. Sliwa,⁵⁴ J.R. Smith,⁷ F.D. Snider,¹⁵ A. Soha,¹⁵ S. Somalwar,⁵⁰ V. Sorin,⁴ P. Squillacioti,⁴⁴
 M. Stancari,¹⁵ M. Stanitzki,⁵⁹ R. St. Denis,¹⁹ B. Stelzer,³¹ O. Stelzer-Chilton,³¹ D. Stentz,³⁶ J. Strologas,³⁵
 G.L. Strycker,³² Y. Sudo,⁵³ A. Sukhanov,¹⁶ I. Suslov,¹³ K. Takemasa,⁵³ Y. Takeuchi,⁵³ J. Tang,¹¹ M. Tecchio,³²
 P.K. Teng,¹ J. Thom^{f,15} J. Thome,¹⁰ G.A. Thompson,²² E. Thomson,⁴³ P. Ttito-Guzmán,²⁹ S. Tkaczyk,¹⁵
 D. Toback,⁵¹ S. Tokar,¹² K. Tollefson,³³ T. Tomura,⁵³ D. Tonelli,¹⁵ S. Torre,¹⁷ D. Torretta,¹⁵ P. Totaro,⁴¹
 M. Trovato^{ee,44} Y. Tu,⁴³ F. Ukegawa,⁵³ S. Uozumi,²⁵ A. Varganov,³² F. Vázquez^{k,16} G. Velev,¹⁵ C. Vellidis,³
 M. Vidal,²⁹ I. Vila,⁹ R. Vilar,⁹ J. Vizán,⁹ M. Vogel,³⁵ G. Volpi^{cc,44} P. Wagner,⁴³ R.L. Wagner,¹⁵ T. Wakisaka,³⁹
 R. Wallny,⁸ S.M. Wang,¹ A. Warburton,³¹ D. Waters,²⁸ M. Weinberger,⁵¹ W.C. Wester III,¹⁵ B. Whitehouse,⁵⁴
 D. Whiteson^{b,43} A.B. Wicklund,² E. Wicklund,¹⁵ S. Wilbur,¹¹ F. Wick,²⁴ H.H. Williams,⁴³ J.S. Wilson,³⁷
 P. Wilson,¹⁵ B.L. Winer,³⁷ P. Wittich^{f,15} S. Wolbers,¹⁵ H. Wolfe,³⁷ T. Wright,³² X. Wu,¹⁸ Z. Wu,⁵ K. Yamamoto,³⁹
 J. Yamaoka,¹⁴ T. Yang,¹⁵ U.K. Yang^{p,11} Y.C. Yang,²⁵ W.-M. Yao,²⁶ G.P. Yeh,¹⁵ K. Yi^{m,15} J. Yoh,¹⁵ K. Yorita,⁵⁶
 T. Yoshida^{j,39} G.B. Yu,¹⁴ I. Yu,²⁵ S.S. Yu,¹⁵ J.C. Yun,¹⁵ A. Zanetti,⁵² Y. Zeng,¹⁴ and S. Zucchelli^{aa6}

(CDF Collaboration)[†]

¹*Institute of Physics, Academia Sinica, Taipei, Taiwan 11529, Republic of China*

²*Argonne National Laboratory, Argonne, Illinois 60439, USA*

³*University of Athens, 157 71 Athens, Greece*

⁴*Institut de Física d'Altes Energies, ICREA, Universitat Autònoma de Barcelona, E-08193, Bellaterra (Barcelona), Spain*

⁵*Baylor University, Waco, Texas 76798, USA*

⁶*Istituto Nazionale di Fisica Nucleare Bologna, ^{aa}University of Bologna, I-40127 Bologna, Italy*

⁷*University of California, Davis, Davis, California 95616, USA*

⁸*University of California, Los Angeles, Los Angeles, California 90024, USA*

⁹*Instituto de Física de Cantabria, CSIC-University of Cantabria, 39005 Santander, Spain*

¹⁰*Carnegie Mellon University, Pittsburgh, Pennsylvania 15213, USA*

¹¹*Enrico Fermi Institute, University of Chicago, Chicago, Illinois 60637, USA*

¹²*Comenius University, 842 48 Bratislava, Slovakia; Institute of Experimental Physics, 040 01 Kosice, Slovakia*

¹³*Joint Institute for Nuclear Research, RU-141980 Dubna, Russia*

¹⁴*Duke University, Durham, North Carolina 27708, USA*

¹⁵*Fermi National Accelerator Laboratory, Batavia, Illinois 60510, USA*

¹⁶*University of Florida, Gainesville, Florida 32611, USA*

¹⁷*Laboratori Nazionali di Frascati, Istituto Nazionale di Fisica Nucleare, I-00044 Frascati, Italy*

¹⁸*University of Geneva, CH-1211 Geneva 4, Switzerland*

¹⁹*Glasgow University, Glasgow G12 8QQ, United Kingdom*

²⁰*Harvard University, Cambridge, Massachusetts 02138, USA*

²¹*Division of High Energy Physics, Department of Physics, University of Helsinki and Helsinki Institute of Physics, FIN-00014, Helsinki, Finland*

²²*University of Illinois, Urbana, Illinois 61801, USA*

²³*The Johns Hopkins University, Baltimore, Maryland 21218, USA*

²⁴*Institut für Experimentelle Kernphysik, Karlsruhe Institute of Technology, D-76131 Karlsruhe, Germany*

²⁵*Center for High Energy Physics: Kyungpook National University, Daegu 702-701, Korea; Seoul National University, Seoul 151-742, Korea; Sungkyunkwan University, Suwon 440-746, Korea; Korea Institute of Science and Technology Information, Daejeon 305-806, Korea; Chonnam National University, Gwangju 500-757, Korea; Chonbuk National University, Jeonju 561-756, Korea*

²⁶*Ernest Orlando Lawrence Berkeley National Laboratory, Berkeley, California 94720, USA*

²⁷*University of Liverpool, Liverpool L69 7ZE, United Kingdom*

²⁸*University College London, London WC1E 6BT, United Kingdom*

²⁹*Centro de Investigaciones Energéticas Medioambientales y Tecnológicas, E-28040 Madrid, Spain*

³⁰*Massachusetts Institute of Technology, Cambridge, Massachusetts 02139, USA*

³¹*Institute of Particle Physics: McGill University, Montréal, Québec, Canada H3A 2T8; Simon Fraser University, Burnaby, British Columbia, Canada V5A 1S6; University of Toronto, Toronto, Ontario, Canada M5S 1A7; and TRIUMF, Vancouver, British Columbia, Canada V6T 2A3*

- ³² *University of Michigan, Ann Arbor, Michigan 48109, USA*
³³ *Michigan State University, East Lansing, Michigan 48824, USA*
³⁴ *Institution for Theoretical and Experimental Physics, ITEP, Moscow 117259, Russia*
³⁵ *University of New Mexico, Albuquerque, New Mexico 87131, USA*
³⁶ *Northwestern University, Evanston, Illinois 60208, USA*
³⁷ *The Ohio State University, Columbus, Ohio 43210, USA*
³⁸ *Okayama University, Okayama 700-8530, Japan*
³⁹ *Osaka City University, Osaka 588, Japan*
⁴⁰ *University of Oxford, Oxford OX1 3RH, United Kingdom*
⁴¹ *Istituto Nazionale di Fisica Nucleare, Sezione di Padova-Trento, ^{bb}University of Padova, I-35131 Padova, Italy*
⁴² *LPNHE, Universite Pierre et Marie Curie/IN2P3-CNRS, UMR7585, Paris, F-75252 France*
⁴³ *University of Pennsylvania, Philadelphia, Pennsylvania 19104, USA*
⁴⁴ *Istituto Nazionale di Fisica Nucleare Pisa, ^{cc}University of Pisa,*
^{dd} *University of Siena and ^{ee}Scuola Normale Superiore, I-56127 Pisa, Italy*
⁴⁵ *University of Pittsburgh, Pittsburgh, Pennsylvania 15260, USA*
⁴⁶ *Purdue University, West Lafayette, Indiana 47907, USA*
⁴⁷ *University of Rochester, Rochester, New York 14627, USA*
⁴⁸ *The Rockefeller University, New York, New York 10065, USA*
⁴⁹ *Istituto Nazionale di Fisica Nucleare, Sezione di Roma 1, ^{ff}Sapienza Università di Roma, I-00185 Roma, Italy*
⁵⁰ *Rutgers University, Piscataway, New Jersey 08855, USA*
⁵¹ *Texas A&M University, College Station, Texas 77843, USA*
⁵² *Istituto Nazionale di Fisica Nucleare Trieste/Udine, I-34100 Trieste, ^{gg}University of Udine, I-33100 Udine, Italy*
⁵³ *University of Tsukuba, Tsukuba, Ibaraki 305, Japan*
⁵⁴ *Tufts University, Medford, Massachusetts 02155, USA*
⁵⁵ *University of Virginia, Charlottesville, Virginia 22906, USA*
⁵⁶ *Waseda University, Tokyo 169, Japan*
⁵⁷ *Wayne State University, Detroit, Michigan 48201, USA*
⁵⁸ *University of Wisconsin, Madison, Wisconsin 53706, USA*
⁵⁹ *Yale University, New Haven, Connecticut 06520, USA*
(Dated: September 19, 2011)

A search for a narrow Higgs boson resonance in the diphoton mass spectrum is presented based on data corresponding to 7.0 fb^{-1} of integrated luminosity from $p\bar{p}$ collisions at $\sqrt{s} = 1.96 \text{ TeV}$ collected by the CDF experiment. No evidence of such a resonance is observed, and upper limits are set on the cross section times branching ratio of the resonant state as a function of Higgs boson mass. The limits are interpreted in the context of the standard model and one fermiophobic benchmark model where the data exclude fermiophobic Higgs bosons with masses below $114 \text{ GeV}/c^2$ at a 95% Bayesian credibility level.

PACS numbers: 12.38.Qk, 13.85.Rm, 14.80.Cp, 12.60.Jv, 12.60.Fr

In the standard model (SM) of particle physics, the electromagnetic and weak forces are unified into a single theory known as electroweak theory. However, the measured cross sections for electromagnetic and weak interactions differ by several orders of magnitude due to massive W and Z bosons that mediate the weak interactions. These bosons gain mass via electroweak symmetry breaking by way of the Higgs mechanism [1], and the electroweak theory predicts the existence of a boson, known as the Higgs boson, that provides a direct test of the theory.

The SM prediction for the Higgs boson branching ratio into a photon pair $\mathcal{B}(H \rightarrow \gamma\gamma)$ is extremely small, reaching a maximal value of only about 0.2% for a Higgs boson mass $m_H = 120 \text{ GeV}/c^2$ [2]. Even so, a search using the diphoton final state is appealing due to its better mass resolution and reconstruction efficiency relative to dominant decay modes involving b quarks. The $H \rightarrow \gamma\gamma$ channel provides its greatest sensitivity for Higgs boson

masses between 110 and $140 \text{ GeV}/c^2$, contributing in a region most useful to combined Tevatron Higgs boson searches [3] and overlapping with a region preferred by electroweak constraints [4]. In addition, in “fermiophobic” Higgs boson models, where the coupling of the Higgs boson to fermions is suppressed, the diphoton decay can be greatly enhanced [5].

The Collider Detector at Fermilab (CDF) and D0 experiments at the Tevatron have searched for both a SM Higgs boson and a fermiophobic Higgs boson h_f decaying to two photons [6–8]. The D0 experiment recently set 95% confidence level (C.L.) upper limits on the cross section times branching ratio $\sigma \times \mathcal{B}(H \rightarrow \gamma\gamma)$ relative to the SM prediction and on $\mathcal{B}(h_f \rightarrow \gamma\gamma)$ using data corresponding to an integrated luminosity \mathcal{L} of 8.2 fb^{-1} [9]. The h_f result sets a lower limit on m_{h_f} of $112.9 \text{ GeV}/c^2$, a more stringent limit than that of $109.7 \text{ GeV}/c^2$ obtained from combined searches at the LEP electron-positron collider at CERN [10]. Previously, the CDF experiment set

95% C.L. upper limits on $\mathcal{B}(h_f \rightarrow \gamma\gamma)$ with data corresponding to $\mathcal{L} = 3.0 \text{ fb}^{-1}$, resulting in an exclusion of m_{h_f} below $106 \text{ GeV}/c^2$ [11].

In this Letter, we present a search of the diphoton mass distribution from CDF data for a narrow resonance that could reveal the presence of a SM or fermiophobic Higgs boson. This analysis, which uses more than twice the integrated luminosity of the previous CDF h_f analysis [11], implements new techniques to improve the identification of photons and yields a new, improved lower limit on the fermiophobic Higgs boson mass. In addition, this is the first search for the SM Higgs boson at CDF using $H \rightarrow \gamma\gamma$ decays from Run II data.

The SM Higgs production mechanisms considered in this study are gluon fusion (GF), associated production (VH) where a Higgs boson is produced in association with a W or Z boson, and vector boson fusion (VBF) with cross sections of 1072.3 fb [12, 13], 240.3 fb [14], and 72.7 fb [15], respectively, for $m_H = 120 \text{ GeV}/c^2$. A benchmark fermiophobic model is considered in which the Higgs boson does not couple to fermions, yet retains its SM couplings to bosons [16]. In this model, the GF process is suppressed and the fermiophobic Higgs boson production is dominated by VH and VBF. Table II gives the predicted $\mathcal{B}(h_f \rightarrow \gamma\gamma)$ for this model.

We use the CDF II detector [17] to identify photon candidate events produced in $p\bar{p}$ collisions at $\sqrt{s} = 1.96 \text{ TeV}$. The silicon vertex tracker [18] and the central outer tracker (COT) [19], contained within a 1.4 T axial magnetic field, measure the trajectories of charged particles and determine their momenta. Particles that pass through the COT reach the electromagnetic (EM) and hadronic calorimeters [20–22], which are divided into two regions: central ($|\eta| < 1.1$) [23] and forward or “plug” ($1.1 < |\eta| < 3.6$). The EM calorimeters contain fine-grained shower maximum detectors [24], which measure the shower shape and centroid position in the two dimensions transverse to the direction of the shower development.

Events with two photon candidates are selected and the data are divided into four independent subsamples according to the position and type of the photons. In central-central (CC) events, both photon candidates are located within the fiducial region of the central EM calorimeter ($|\eta| < 1.05$); in central-plug (CP) events, one photon candidate is located in this region and the other is in the fiducial region of the plug calorimeter ($1.2 < |\eta| < 2.8$); in central-central events with a conversion (C’C), both photon candidates are in the central region, but one photon converts and is reconstructed from its e^+e^- decay products; in central-plug events with a conversion (C’P), there is one central conversion candidate together with a plug photon candidate.

The events are selected by a three-level trigger system that requires an isolated cluster of energy deposited in the EM calorimeter with a transverse energy $E_T >$

25 GeV [25]. The trigger efficiency for events accepted into the final sample is determined from simulation and found to be essentially 100% for the most sensitive event category (CC) and above 90% for all other categories.

A set of selection criteria is used to remove background events and to identify high-energy photon candidates for this analysis. All reconstructed photon candidates are required to have $E_T > 15 \text{ GeV}$. Plug photon candidates are identified using standard CDF requirements described elsewhere [26, 27]. A neural network (NN) technique is used to identify photons in the central region, published for the first time in this Letter. Central photon candidates are first required to satisfy loose selection requirements as described in Ref. [28]. After additional track requirements are applied to remove electrons, the remaining candidates are required to have a NN output value above a threshold that is selected to maximize $H \rightarrow \gamma\gamma$ sensitivity. As more than half of the events in the data with two photon candidates contain either one or two jets misidentified as a prompt photon [29], the NN discriminant is trained using photon and jet Monte Carlo (MC) samples and constructed from several detector variables that distinguish true photons from these jet backgrounds [30]. These variables include the ratio of energy in the shower maximum detector to that in the calorimeter cluster associated with the photon, the ratio of hadronic to EM transverse energy (Had/EM), calorimeter and track isolation [28], and a χ^2 value calculated by comparing the measured transverse shower profile to that of a single EM shower [31]. This NN method increases the photon signal efficiency by $\sim 5\%$ and background rejection by $\sim 12\%$ compared to the standard selection requirements for central photons [28], which improves $H \rightarrow \gamma\gamma$ sensitivity by about 9%.

As photons pass through the CDF detector material, EM interactions with a nucleus cause about 15% of central photons to convert into an electron-positron pair. In order to recover these conversion photons, we search for a central electron with a nearby track corresponding to a particle of opposite charge. The proximity of the two tracks is first determined by requiring the transverse distance between the two tracks to be less than 0.2 cm at the radial location where they are parallel. The difference in $\cot\theta$ between the two tracks must be less than 0.04, where $\cot\theta = p_z/p_T$. Backgrounds are further removed by requiring the ratio of E_T to p_T of the reconstructed conversion photon to be between $0.1c$ and $1.9c$, and calorimeter isolation to be less than 2.6 GeV , where cut boundaries are optimized to maximize $H \rightarrow \gamma\gamma$ sensitivity. The direction of the conversion photon’s momentum is obtained by taking the vector sum of the individual track momenta. Better $H \rightarrow \gamma\gamma$ mass resolution is obtained, however, by setting the total momentum to be the conversion photon’s energy obtained from EM calorimeters. Reconstruction of photon conversions in this analysis provides an improvement of about 13%

TABLE I. Efficiency times detector acceptance (ϵA) for signal events (in %) in each event category ($m_H = 120 \text{ GeV}/c^2$). Results for VH and VBF are shown for the high/medium/low $p_T^{\gamma\gamma}$ regions defined for the h_f search as described in the text. The sum of the values across $p_T^{\gamma\gamma}$ regions, together with the GF value, is used for the SM Higgs boson search.

ϵA (%)	GF	VH	VBF
CC	10.0	4.9 / 3.8 / 1.9	4.2 / 4.6 / 2.6
CP	12.2	4.2 / 4.8 / 2.5	3.6 / 5.1 / 3.1
C'C	2.4	1.0 / 0.9 / 0.4	0.9 / 1.0 / 0.6
C'P	1.5	0.4 / 0.5 / 0.3	0.4 / 0.6 / 0.3
Total	26.2	10.6 / 10.0 / 5.2	9.1 / 11.3 / 6.6

in sensitivity to a Higgs boson signal [32].

The above selection criteria define an inclusive diphoton sample for the SM Higgs boson search. In order to improve sensitivity for the fermiophobic Higgs boson search, the event selection is extended by taking advantage of the final state features present in the VH and VBF processes. Because the Higgs boson from these processes will be produced with a W or Z boson, or with two jets, the transverse momentum of the diphoton system $p_T^{\gamma\gamma}$ is generally higher relative to the diphoton backgrounds. A requirement of $p_T^{\gamma\gamma} > 75 \text{ GeV}/c$ forms a region of high h_f sensitivity, retaining roughly 30% of the signal while removing 99.5% of the background [11]. Two lower $p_T^{\gamma\gamma}$ regions are additionally included and provide about 15% more h_f sensitivity: $p_T^{\gamma\gamma} < 35 \text{ GeV}/c$ and $35 \text{ GeV}/c < p_T^{\gamma\gamma} < 75 \text{ GeV}/c$. With four diphoton categories (CC, CP, C'C, and C'P) and three $p_T^{\gamma\gamma}$ regions, twelve independent channels are included for the fermiophobic Higgs boson search.

The efficiency times detector acceptance for signal events given in Table I is calculated using PYTHIA [33] MC event samples, which are generated as described in Ref. [11]. Corrections in the photon identification (ID) efficiencies due to imperfections in the detector simulation are derived using electrons from Z boson decays [11]. For central conversions, a study of $Z \rightarrow e^\pm + \text{trident}$ events in data and MC is used to obtain a systematic uncertainty of 7% on the efficiency of conversion identification, where a trident is defined as an electron that radiates a photon via bremsstrahlung which then converts to an electron-positron pair ($e^\mp \gamma \rightarrow e^\mp e^+ e^-$).

The largest systematic uncertainties on the expected number of Higgs boson events arise from the conversion ID efficiency (7%), the integrated luminosity measurement (6%), varying the parton distribution functions used in PYTHIA (up to 5%) [34, 35], varying the parameters that control the amount of initial and final state radiation from the parton shower model of PYTHIA (about 4%) [36], and the PYTHIA modeling of the shape of the $p_T^{\gamma\gamma}$ distribution for the h_f signal (up to 4%). The latter uncertainty is only for VH and VBF used in the fermiophobic search and was obtained by studying the effect

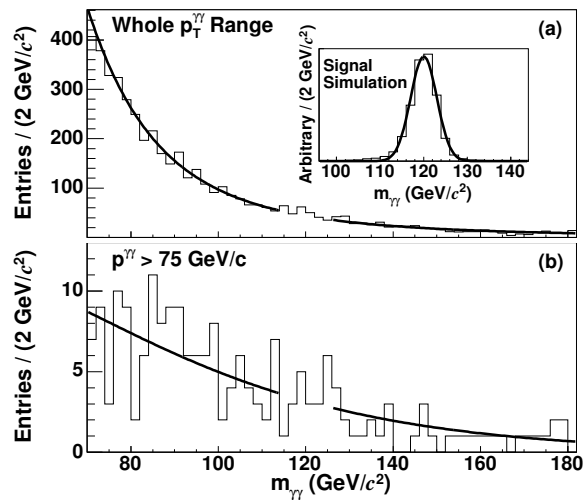


FIG. 1. The invariant mass distribution of the data for CC photon pairs is shown in (a) for the entire $p_T^{\gamma\gamma}$ region used in the SM Higgs boson search and (b) for the highest $p_T^{\gamma\gamma}$ region (the most sensitive region) used in the h_f search. Each distribution shows a fit to the data for the hypothesis of a m_H of $120 \text{ GeV}/c^2$. The gap in the fit centered at $120 \text{ GeV}/c^2$ represents the signal region for this mass point that was excluded from the fit. The expected shape of the signal from simulation is shown in the inset of (a).

on the acceptance from the differences in the shape of the $p_T^{\gamma\gamma}$ distribution from PYTHIA and from leading-order and next-to-leading-order calculations [37]. Finally, we include uncertainties from the photon ID efficiency (up to 4%) and the EM energy scale (less than 1%).

The decay of a Higgs boson into a photon pair would appear as a very narrow peak in the invariant mass distribution of the two photons (see Fig. 1 as an example for the CC sample). The diphoton mass resolution, as determined from simulation and checked using $Z \rightarrow e^+e^-$ decays in data, is better than $3 \text{ GeV}/c^2$ for the Higgs boson mass regions and diphoton channels studied here and is limited by the energy resolution of the EM calorimeters [38]. The mass resolution is also sensitive to the selection of the correct primary vertex of the $p\bar{p}$ interaction, determined by selecting the vertex with the highest sum of associated track momenta. The locations of the vertex and EM energy cluster are used to derive the photon's momentum. For GF (VH and VBF) signal samples, the primary vertex is misidentified in roughly 16% (4%) of non-conversion channel (CC and CP) events, which degrades the resolution of the reconstructed Higgs boson mass [39]. This effect is studied using Z decays in the data and found to be well modeled in the simulation.

The total background prediction is estimated from a fit made to the data using a binned log-likelihood ($\log \ell$) method [40]. The fit is performed for each m_H hypothesis in $5 \text{ GeV}/c^2$ steps from 100 to $150 \text{ GeV}/c^2$. At each

TABLE II. Expected and observed 95% C.L. upper limits on the production cross section times branching ratio relative to the SM prediction, the production cross section times branching ratio with theoretical cross section uncertainties removed, and the h_f branching ratio. The fermiophobic benchmark model prediction for $\mathcal{B}(h_f \rightarrow \gamma\gamma)$ is also shown for comparison.

	m_H (GeV/ c^2)	100	105	110	115	120	125	130	135	140	145	150
$\sigma \times \mathcal{B}(H \rightarrow \gamma\gamma)/\text{SM}$	Expected	16.4	14.8	14.2	13.8	13.3	13.6	14.4	15.8	17.7	20.8	27.5
	Observed	15.1	13.9	8.5	14.6	28.7	19.2	19.2	14.8	23.1	21.9	21.4
$\sigma \times \mathcal{B}(H \rightarrow \gamma\gamma)$ (fb)	Expected	57.3	50.8	47.9	43.2	39.0	36.0	32.8	30.6	28.5	26.7	26.1
	Observed	52.9	47.8	28.8	44.8	84.4	50.4	44.7	29.4	36.9	28.0	20.2
$\mathcal{B}(h_f \rightarrow \gamma\gamma)$ (%)	Expected	4.4	4.9	5.2	5.8	6.0	6.4	6.8	7.4	7.7	8.1	8.7
	Observed	4.8	5.4	2.8	4.2	7.3	5.5	6.6	6.6	5.7	7.8	8.1
	Fermiophobic Prediction	18.2	10.6	6.2	3.8	2.8	2.2	1.9	1.2	0.6	0.3	0.2

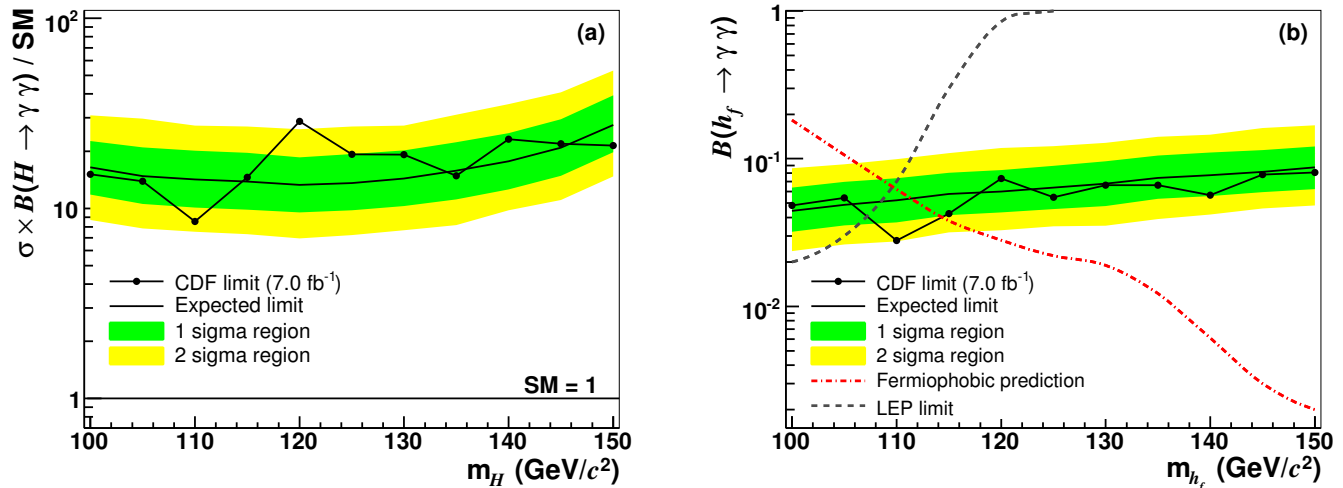


FIG. 2. (a) As a function of m_H , the 95% C.L. upper limit on cross section times branching ratio for the SM Higgs boson decay to two photons, relative to the SM prediction. (b) The 95% C.L. upper limit on the branching ratio for the fermiophobic Higgs boson decay to two photons, as a function of m_{h_f} . For reference, the 95% C.L. limits from LEP are also included. The shaded regions represent the 1σ and 2σ probability of fluctuations of the observed limit away from the expected limit based on the distribution of simulated experimental outcomes.

step a $12 \text{ GeV}/c^2$ mass window centered on the point is excluded, where $12 \text{ GeV}/c^2$ is chosen to include 95% of the signal. Fits for a m_H hypothesis of $120 \text{ GeV}/c^2$ are shown in Fig. 1. The statistical uncertainties on the total background in the signal region, taken from the fit, are 8% or less for the channels associated with the SM Higgs boson search and 12% or less for the channels associated with the fermiophobic Higgs boson search (except for the high- $p_T^{\gamma\gamma}$ bins with conversion photons, where it is 27%).

No obvious evidence of a narrow peak or any other anomalous structure is visible in the diphoton mass spectrum. We calculate a Bayesian C.L. limit for each Higgs boson mass hypothesis based on a combination of likelihoods from the mass distributions for all channels in the $12 \text{ GeV}/c^2$ signal region. We use a flat prior in $\sigma \times \mathcal{B}(H \rightarrow \gamma\gamma)$ and integrate over the priors for the systematic uncertainties. A 95% C.L. limit is determined such that 95% of the posterior density for $\sigma \times \mathcal{B}(H \rightarrow \gamma\gamma)$ falls below the limit [41]. The expected 95% C.L. lim-

its are calculated assuming no signal, based on expected backgrounds only, as the median of 2000 simulated experiments. The observed 95% C.L. on $\sigma \times \mathcal{B}(H \rightarrow \gamma\gamma)$ are calculated from the data. The limit results are displayed in Table II and graphically in Fig. 2. For a SM Higgs boson, the results are shown relative to the theory prediction, where theoretical cross section uncertainties of 14% on the GF process, 6% on the VH process, and 5% on the VBF process are included in the limit calculation [42, 43]. Limits are also provided on $\sigma \times \mathcal{B}(H \rightarrow \gamma\gamma)$ without including theoretical cross section uncertainties. The inclusion of systematic uncertainties in the SM (fermiophobic) limit calculation degrades the limit on $\sigma \times \mathcal{B}(H \rightarrow \gamma\gamma)$ by 15% (9%) where the effect of the uncertainty on the background estimate is dominant at 10% (6%).

For the SM limit at $m_H = 120 \text{ GeV}/c^2$, we observe a deviation of greater than 2.5σ from the expectation [44]. After accounting for the trials factor associated with per-

forming the search at 11 mass points, the significance of this discrepancy decreases to less than 2σ . When the analysis is optimized for the fermiophobic benchmark model, no excess is observed. For the h_f model, SM cross sections and uncertainties are assumed (GF excluded) and used to convert limits on $\sigma \times \mathcal{B}(h_f \rightarrow \gamma\gamma)$ into limits on $\mathcal{B}(h_f \rightarrow \gamma\gamma)$. We obtain a limit of $m_{h_f} < 114 \text{ GeV}/c^2$ by linear interpolation between the sampled values of m_{h_f} based on the intersection of the observed limit and the model prediction.

This Letter presents the results of a search for a narrow resonance in the diphoton mass spectrum using data taken by the CDF II detector at the Tevatron. We have improved upon the previous CDF analysis by implementing a neural network discriminant to improve central photon identification, recovering central photons that have converted to an e^+e^- pair, and more than doubling the amount of data analyzed. There is no significant evidence of a resonance in the data. Limits are placed on the production cross section times branching ratio for Higgs boson decay into a photon pair and compared to the predictions of the standard model and a benchmark fermiophobic model. The latter results in a limit on the fermiophobic Higgs boson mass of $m_{h_f} > 114 \text{ GeV}/c^2$ at the 95% C.L., which is the strongest to date on this model by a single experiment.

We thank the Fermilab staff and the technical staffs of the participating institutions for their vital contributions. This work was supported by the U.S. Department of Energy and National Science Foundation; the Italian Istituto Nazionale di Fisica Nucleare; the Ministry of Education, Culture, Sports, Science and Technology of Japan; the Natural Sciences and Engineering Research Council of Canada; the National Science Council of the Republic of China; the Swiss National Science Foundation; the A.P. Sloan Foundation; the Bundesministerium für Bildung und Forschung, Germany; the Korean World Class University Program, the National Research Foundation of Korea; the Science and Technology Facilities Council and the Royal Society, UK; the Institut National de Physique Nucleaire et Physique des Particules/CNRS; the Russian Foundation for Basic Research; the Ministerio de Ciencia e Innovación, and Programa Consolider-Ingenio 2010, Spain; the Slovak R&D Agency; the Academy of Finland; and the Australian Research Council (ARC).

* Deceased

† With visitors from ^aIstituto Nazionale di Fisica Nucleare, Sezione di Cagliari, 09042 Monserrato (Cagliari), Italy, ^bUniversity of CA Irvine, Irvine, CA 92697, USA, ^cUniversity of CA Santa Barbara, Santa Barbara, CA 93106, USA, ^dUniversity of CA Santa Cruz, Santa Cruz, CA 95064, USA, ^eCERN, CH-1211 Geneva, Switzerland,

- ^fCornell University, Ithaca, NY 14853, USA, ^gUniversity of Cyprus, Nicosia CY-1678, Cyprus, ^hOffice of Science, U.S. Department of Energy, Washington, DC 20585, USA, ⁱUniversity College Dublin, Dublin 4, Ireland, ^jUniversity of Fukui, Fukui City, Fukui Prefecture, Japan 910-0017, ^kUniversidad Iberoamericana, Mexico D.F., Mexico, ^lIowa State University, Ames, IA 50011, USA, ^mUniversity of Iowa, Iowa City, IA 52242, USA, ⁿKinki University, Higashi-Osaka City, Japan 577-8502, ^oKansas State University, Manhattan, KS 66506, USA, ^pUniversity of Manchester, Manchester M13 9PL, United Kingdom, ^qQueen Mary, University of London, London, E1 4NS, United Kingdom, ^rUniversity of Melbourne, Victoria 3010, Australia, ^sMuons, Inc., Batavia, IL 60510, USA, ^tNagasaki Institute of Applied Science, Nagasaki, Japan, ^uNational Research Nuclear University, Moscow, Russia, ^vUniversity of Notre Dame, Notre Dame, IN 46556, USA, ^wUniversidad de Oviedo, E-33007 Oviedo, Spain, ^xTexas Tech University, Lubbock, TX 79609, USA, ^yUniversidad Tecnica Federico Santa Maria, 110v Valparaiso, Chile, ^zYarmouk University, Irbid 211-63, Jordan, ^{hh}On leave from J. Stefan Institute, Ljubljana, Slovenia.
- [1] P. W. Higgs, *Phys. Rev. Lett.* **13**, 508 (1964); G. S. Guralnik, C. R. Hagen, and T. W. B. Kibble, *Phys. Rev. Lett.* **13**, 585 (1964); F. Englert and R. Brout, *Phys. Rev. Lett.* **13**, 321 (1964).
- [2] A. Djouadi, J. Kalinowski, and M. Spira, *Comput. Phys. Commun.* **108**, 56 (1998).
- [3] Tevatron New Phenomena and Higgs Working Group (CDF and D0 Collaborations), [arXiv:1107.5518](https://arxiv.org/abs/1107.5518).
- [4] LEP, Tevatron, and SLD Electroweak Working Groups, [arXiv:1012.2367](https://arxiv.org/abs/1012.2367).
- [5] H. E. Haber, G. L. Kane, and T. Sterling, *Nucl. Phys. B* **161**, 493 (1979); J. F. Gunion, R. Vega, and J. Wudka, *Phys. Rev. D* **42**, 1673 (1990); V. Barger, N. G. Deshpande, J. L. Hewett, and T. G. Rizzo, [arXiv:hep-ph/9211234](https://arxiv.org/abs/hep-ph/9211234); J.-L. Basdevant, E. L. Berger, D. Dicus, C. Kao, and S. Willenbrock, *Phys. Lett. B* **313**, 402 (1993); B. A. Dobrescu, *Phys. Rev. D* **63**, 015004 (2000); G. Landsberg and K. T. Matchev, *Phys. Rev. D* **62**, 035004 (2000); S. Mrenna and J. Wells, *Phys. Rev. D* **63**, 015006 (2001); A. Barroso, L. Brücher, and R. Santos, *Phys. Rev. D* **60**, 035005 (1999).
- [6] T. Affolder *et al.* (CDF Collaboration), *Phys. Rev. D* **64**, 092002 (2001).
- [7] B. Abbott *et al.* (D0 Collaboration), *Phys. Rev. Lett.* **82**, 2244 (1999).
- [8] V. M. Abazov *et al.* (D0 Collaboration), *Phys. Rev. Lett.* **101**, 051801 (2008).
- [9] V. M. Abazov *et al.* (D0 Collaboration), [arXiv:1107.4587](https://arxiv.org/abs/1107.4587).
- [10] A. Rosca (LEP Collaborations), [arXiv:hep-ex/0212038](https://arxiv.org/abs/hep-ex/0212038).
- [11] T. Aaltonen *et al.* (CDF Collaboration), *Phys. Rev. Lett.* **103**, 061803 (2009).
- [12] C. Anastasiou, R. Boughezal, and F. Petriello, *J. High Energy Phys.* **0904**, 003 (2009).
- [13] D. de Florian and M. Grazzini, *Phys. Lett. B* **674**, 291 (2009).
- [14] J. Baglio and A. Djouadi, *J. High Energy Phys.* **1010**, 064 (2010).
- [15] P. Bolzoni, F. Maltoni, S.-O. Moch, and M. Zaro, *Phys. Rev. Lett.* **105**, 011801 (2010).
- [16] A. G. Akeroyd, *Phys. Lett. B* **368**, 89 (1996).

- [17] D. Acosta *et al.* (CDF Collaboration), *Phys. Rev. D* **71**, 032001 (2005).
- [18] A. Sill (CDF Collaboration), *Nucl. Instrum. Methods Phys. Res., Sect. A* **447**, 1 (2000).
- [19] T. Affolder *et al.*, *Nucl. Instrum. Methods Phys. Res., Sect. A* **526**, 249 (2004).
- [20] L. Balka *et al.*, *Nucl. Instrum. Methods Phys. Res., Sect. A* **267**, 272 (1988).
- [21] S. Bertolucci *et al.*, *Nucl. Instrum. Methods Phys. Res., Sect. A* **267**, 301 (1988).
- [22] M. Albrow *et al.*, *Nucl. Instrum. Methods Phys. Res., Sect. A* **480**, 524 (2002).
- [23] CDF uses a cylindrical coordinate system with $+z$ in the proton beam direction. θ and ϕ are the polar and azimuthal angles, respectively, and pseudorapidity is $\eta = -\ln \tan(\theta/2)$.
- [24] G. Apollinari, K. Goulianos, P. Melese, and M. Lindgren, *Nucl. Instrum. Methods Phys. Res., Sect. A* **412**, 515 (1998).
- [25] The transverse energy E_T and transverse momentum p_T are defined as $E \sin \theta$ and $|\vec{p}| \sin \theta$, respectively.
- [26] T. Aaltonen *et al.* (CDF Collaboration), *Phys. Rev. Lett.* **99**, 171801 (2007).
- [27] S. Wynne, Ph.D. thesis, University of Liverpool, [Fermilab Report No. FERMILAB-THESIS-2007-17, 2007].
- [28] T. Aaltonen *et al.* (CDF Collaboration), *Phys. Rev. D* **82**, 052005 (2010).
- [29] Typically, this occurs when a jet fragments into a π^0 or η particle that subsequently decays to multiple photons, which are then reconstructed as a single photon.
- [30] The variables also allow the NN method to be applied to electrons, which are used to calibrate ID efficiencies.
- [31] F. Abe *et al.* (CDF Collaboration), *Phys. Rev. D* **48**, 2998 (1993).
- [32] K. Bland, Ph.D. thesis, Baylor University.
- [33] T. Sjöstrand, P. Edén, C. Friberg, L. Lönnblad, G. Miu, S. Mrenna, and E. Norrbin, *Comput. Phys. Commun.* **135**, 238 (2001).
- [34] D. Stump *et al.*, *J. High Energy Phys.* **0410**, 046 (2003).
- [35] D. Bourilkov, R. C. Group, and M. R. Whalley, [arXiv:hep-ph/0605240](https://arxiv.org/abs/hep-ph/0605240).
- [36] We constrain the rate of initial state radiation using Drell-Yan events in data.
- [37] S. Mrenna and C.-P. Yuan, *Phys. Lett. B* **416**, 200 (1998).
- [38] The natural width of the Higgs boson is negligible.
- [39] In CC (CP) events, the resolution degrades by 15 (12)%.
- [40] The combined $p_T^{\gamma\gamma}$ data and low- $p_T^{\gamma\gamma}$ data are fit to a sum of two exponentials multiplied by a fractional degree polynomial, where the degree of one term is a parameter of the fit and the two higher $p_T^{\gamma\gamma}$ regions are fit to a simpler three degree polynomial times an exponential. Channels that have a non-negligible contamination from Z boson decays, additionally include a Breit-Wigner function to model this background.
- [41] K. Nakamura *et al.* (Particle Data Group), *Phys. Lett. G* **37**, 075021 (2010).
- [42] M. Botje *et al.*, [arXiv:1101.0538](https://arxiv.org/abs/1101.0538).
- [43] S. Dittmaier *et al.* (LHC Higgs Cross Section Working Group), [arXiv:1101.0593](https://arxiv.org/abs/1101.0593).
- [44] The LEP Working Group for Higgs Boson Searches (LEP Collaborations), *Phys. Lett. B* **565**, 61 (2003).